

BRAIN COMMUNICATIONS

The dynamic of basal ganglia activity with a multiple covariance method: influences of Parkinson's disease

Clara Rodriguez-Sabate,^{1,2,3} Ingrid Morales,^{1,2} Ricardo Puertas-Avenidaño¹ and  Manuel Rodriguez^{1,2}

The closed-loop cortico-subcortical pathways of basal ganglia have been extensively used to describe the physiology of these centres and to justify the functional disorders of basal ganglia diseases. This approach justifies some experimental and clinical data but not others, and furthermore, it does not include a number of subcortical circuits that may produce a more complex basal ganglia dynamic than that expected for closed-loop linear networks. This work studied the functional connectivity of the main regions of the basal ganglia motor circuit with magnetic resonance imaging and a new method (functional profile method), which can analyse the multiple covariant activity of human basal ganglia. The functional profile method identified the most frequent covariant functional status (profiles) of the basal ganglia motor circuit, ordering them according to their relative frequency and identifying the most frequent successions between profiles (profile transitions). The functional profile method classified profiles as input profiles that accept the information coming from other networks, output profiles involved in the output of processed information to other networks and highly interconnected internal profiles that accept transitions from input profiles and send transitions to output profiles. Profile transitions showed a previously unobserved functional dynamic of human basal ganglia, suggesting that the basal ganglia motor circuit may work as a dynamic multiple covariance network. The number of internal profiles and internal transitions showed a striking decrease in patients with Parkinson's disease, a fact not observed for input and output profiles. This suggests that basal ganglia of patients with Parkinson's disease respond to requirements coming from other neuronal networks, but because the internal processing of information is drastically weakened, its response will be insufficient and perhaps also self-defeating. These marked effects were found in patients with few motor disorders, suggesting that the functional profile method may be an early procedure to detect the first stages of the Parkinson's disease when the motor disorders are not very evident. The multiple covariance activity found presents a complementary point of view to the cortico-subcortical closed-loop model of basal ganglia. The functional profile method may be easily applied to other brain networks, and it may provide additional explanations for the clinical manifestations of other basal ganglia disorders.

1 Laboratory of Neurobiology and Experimental Neurology, Department of Physiology, Faculty of Medicine, University of La Laguna, Tenerife, Canary Islands 28907, Spain

2 Center for Networked Biomedical Research in Neurodegenerative Diseases (CIBERNED), Madrid 28031, Spain

3 Department of Psychiatry, Getafe University Hospital, Madrid 28031, Spain

Correspondence to: Manuel Rodriguez, Laboratory of Neurobiology and Experimental Neurology, Department of Basic Medical Sciences, 38200, Apt. 456, University of La Laguna, Tenerife, Canary Islands, Spain
E-mail: mrdiaz@ull.es

Keywords: basal ganglia; motor cortex; functional connectivity; functional profile method; Parkinson's disease

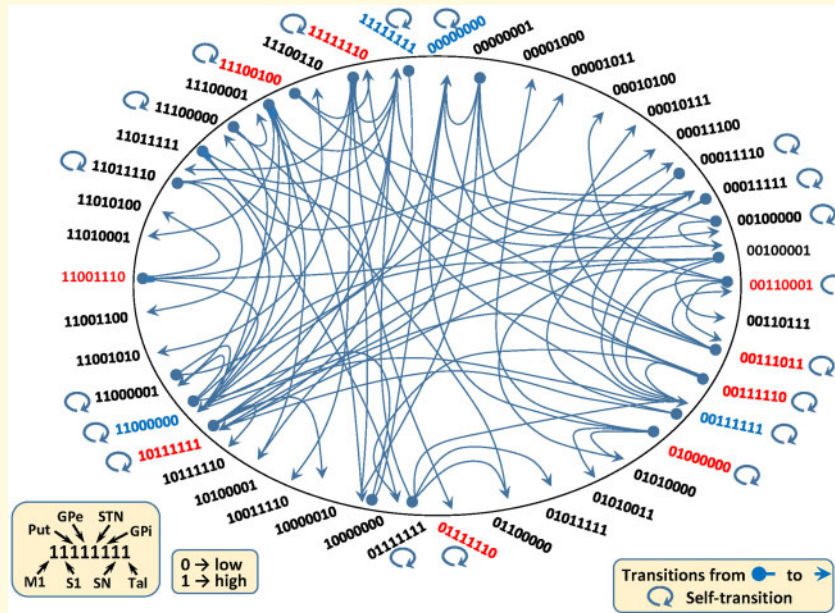
Received July 3, 2019. Revised October 31, 2019. Accepted November 17, 2019. Advance Access publication December 11, 2019

© The Author(s) (2019). Published by Oxford University Press on behalf of the Guarantors of Brain.

This is an Open Access article distributed under the terms of the Creative Commons Attribution Non-Commercial License (<http://creativecommons.org/licenses/by-nc/4.0/>), which permits non-commercial re-use, distribution, and reproduction in any medium, provided the original work is properly cited. For commercial re-use, please contact journals.permissions@oup.com

Abbreviations: BG = basal ganglia; BGmC = basal ganglia motor circuit; BOLD = blood-oxygen-level-dependent imaging; CP = complementary profile; fcMRI = functional connectivity magnetic resonance imaging; FPM = functional profile method; MCA = multiple correspondence analysis; MRI = magnetic resonance imaging; M1 = primary motor cortex; Put = putamen; S1 = primary somatosensory cortex; Tal = motor thalamus

Graphical Abstract



Introduction

Current models of human basal ganglia (BG) are mainly based on experimental studies performed in animals during the 1980s and 90s, studies suggesting that BG are basically arranged in closed-loop networks, which receive cortical inputs and return the processed information to the cortex (Alexander *et al.*, 1986; Albin *et al.*, 1989; DeLong, 1990). One of these loops is the BG motor circuit (BGmC), which moves the information from the primary motor cortex (M1) to the putamen (Put) and from this region to the external globus pallidum, subthalamic nucleus, internal globus pallidum and substantia nigra (SN). The information processed by these regions goes to the anterior thalamus [motor thalamus (Tal)] and then returns to the cortex where it induces a feed-back modulation in the M1 activity. Most models suggest that motor disorders of Parkinson's disease (Canavan *et al.*, 1989; DeLong and Wichmann, 2009; Kravitz *et al.*, 2010; Cui *et al.*, 2013; Cazorla *et al.*, 2014; Yin, 2014, 2016; Neumann *et al.*, 2018; McCutcheon *et al.*, 2019) are induced by changes in the excitatory–inhibitory interactions between the consecutive centres of this closed-loop network. However, this is a simplified view of BG physiology, which does not include a number of BG interactions (Redgrave *et al.*, 1992; McHaffie *et al.*, 2005; Ikemoto *et al.*, 2015; Supplementary Fig. 1) and

which does not explain all motor disorders of Parkinson's disease (Canavan *et al.*, 1989; Soares *et al.*, 2004; DeLong and Wichmann, 2009).

Instead of studying the excitatory–inhibitory interactions between particular BG, this work was aimed at examining the physiological activity of BG as a result of the functional co-activation of their main centres. This approach can be directly performed in the human brain by using magnetic resonance imaging (MRI) methods (functional connectivity MRI, fcMRI; Raichle, 1998; Arthurs and Boniface, 2002; Logothetis, 2002; Logothetis and Wandell, 2004; Raichle and Mintun, 2006; Rodriguez-Sabate *et al.*, 2017b, 2019a). Correlation methods are the most common procedures used to analyse fcMRI data (Fox and Raichle, 2007; Zhang *et al.*, 2010; Rodriguez-Sabate *et al.*, 2017b, 2019b), but they need some requirements (e.g. linear behaviour, normality and stationarity of data) that are not always met in neuronal networks (Eklund *et al.*, 2018; Olszowy *et al.*, 2019). In addition, correlation methods can identify the functional interaction between two nuclei, but they are not the best approach to study the simultaneous interaction of multiple BG areas. Other methods such as the independent component analysis (Damoiseaux *et al.*, 2006; Goebel *et al.*, 2006; Fox and Raichle, 2007) and data-driven sparse general linear model (Lee *et al.*, 2011; Su *et al.*, 2016) can simultaneously work with multiple

regions, but they generally assume a linear interaction between nuclei, which is uncommon in BG (Marceglia *et al.*, 2006; Schroll and Hamker, 2013; Rodriguez-Sabate *et al.*, 2017a) where neurons often display a non-linear dynamic (Rodriguez *et al.*, 2003a, b, c). We have recently introduced a non-linear multifactorial method based on the multiple correspondence analysis (MCA), which showed previously unnoticed multiple covariant behaviour of BG (Rodriguez-Sabate *et al.*, 2017a, 2019a). However, MCA has three key limitations, it is an exploratory method, which does not provide statistical results, it can only identify a small portion of the multi-centre interactions (the number of interactions is always lower than the number of studied nuclei) and it does not provide information about the time dynamic of BG interactions. The present study introduces a new analytical procedure [functional profile method (FPM)] that overcomes these limitations because it does not assume normality or stationarity in fMRI data, it can work with non-linear multiple interactions, it can be used to study the time dynamic of brain interactions and it allows the statistical contrast of results. FPM was used to analyse the dynamic of the functional co-activation of the BGmC and to study the action of Parkinson's disease on this dynamic.

Methods

Participants

Twenty patients with idiopathic Parkinson's disease (10 males and 10 females between 35 and 72 years of age) and no evidence of dementia (tested with the Montreal Cognitive Assessment and the Mini-Mental State Examination) and twenty control subjects (10 males and 10 females between 36 and 69 years of age) with no history of neurological or mental diseases were included in the study. All patients had a diagnosis of idiopathic Parkinson's disease, which was based on their medical history, physical and neurological examinations, response to levodopa or dopaminergic drugs and laboratory tests and MRI scans, which ruled out other diseases (they were diagnosed by two experienced neurologists; F.M. and J.N.L.). The severity of motor disorders was assessed with the Hoehn & Yahr, the Schwab and England and the Unified Parkinson's Disease Rating Scale III scales, which were used to select patients with a short evolution of Parkinson's disease (<2 years) and a slight to moderate motor alteration during the 'on' medication state. The impact of medication on the results was reduced by withdrawing the anti-Parkinson drugs 24 h before the study onset. Written informed consent was provided by all participants, and all procedures were in accordance with the ethical standards of the Declaration of Helsinki and its later amendments or comparable standards. The study was approved by an institutional review board

(Institutional Human Studies Committee of La Laguna University).

Data collection

The basic experimental procedures were similar to those reported in recent studies (Rodriguez-Sabate *et al.*, 2015, 2017b). Blood-oxygen-level-dependent imaging (BOLD) contrast images (4 mm × 4 mm × 4 mm voxels in-plane resolution; echo-planar imaging with repetition time 1.6 s; echo time 21.6 ms; flip angle 90°) were recorded in a block of 200 volumes (volumes 1–10 of the block were removed). fMRI data were co-registered with 3D anatomical images (1 mm × 1 mm × 1 mm voxel resolution; repetition time 7.6 ms; echo time 1.6 ms; flip angle 12°; 250 mm × 250 mm field of view; 256 × 256 sampling matrix). A representative region of interest of each BG was located on a subject-by-subject basis by considering: (i) the Talairach coordinates, (ii) the shape of the nucleus and (iii) the anatomical relationship of the nucleus with neighbouring structures. All regions were identified in coronal slices located 4–27 mm posterior to the anterior commissure and according to a previously reported procedure (Rodriguez-Sabate *et al.*, 2017b). All data sets were normalized to the Talairach space.

Data preprocessing

The data preprocessing included a slice scan time correction, a 3D motion correction and a time filter, which eliminates frequencies <0.009 Hz. Studies with images showing a displacement of >0.5 mm or a rotation of >0.5° were removed. No spatial smoothing was performed. Residual motion artefacts and physiological signals unrelated to neural activity (e.g. respiration, cardiac activity) were removed by regressing the BOLD signals recorded throughout the brain with the mean average of the BOLD signals recorded in white matter and brain ventricles (Jo *et al.*, 2013; Power *et al.*, 2014).

Functional profile method

To identify the most frequent coinciding patterns of BG activity (BG activity profiles), BOLD data were normalized and binarized. Data were normalized by multiplying them by 100 and dividing the result by the mean average value of all the data recorded in the same area of the same subject. Thus, the normalized BOLD data of an area always fluctuated ~100 and represent, in percentage terms, the fluctuation of the BOLD signal around the mean BOLD value of the region of interest, which represents the functional activity of the area (see Fig. 1A). The binarization was performed by replacing each normalized data >100 with the number 1 and those ≤100 with the number 0 (see Fig. 1B). Thus, the functional status of the BGmC at each time point was compiled in a single byte [the first-left bit occupied by the M1 and the following bits were occupied by the primary somatosensory cortex

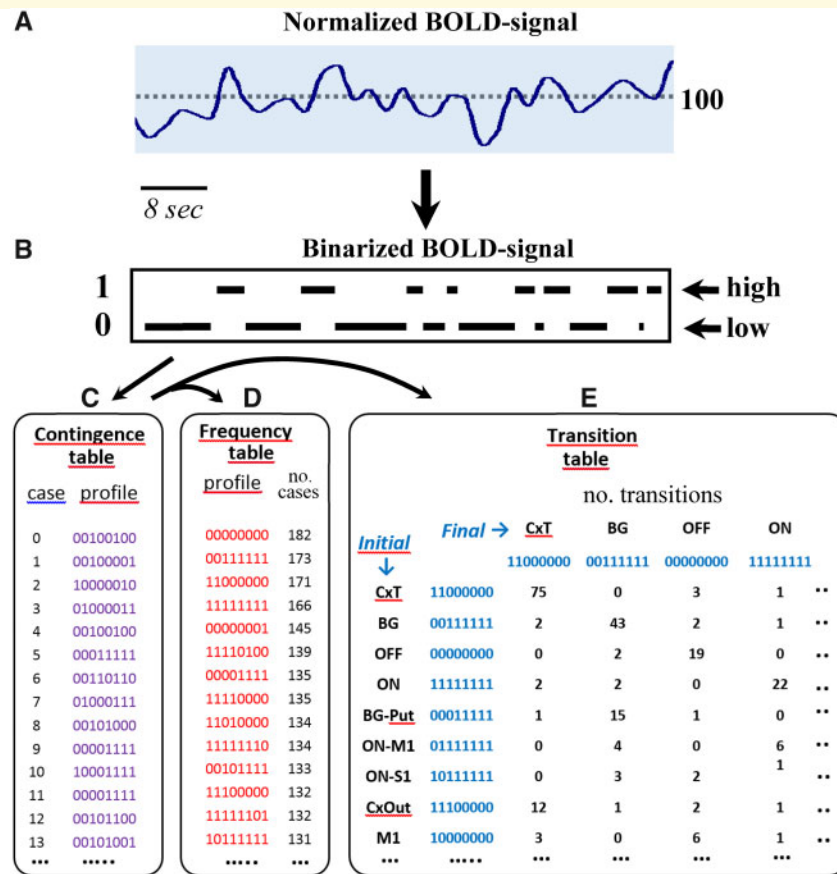


Figure 1 FPM. The BOLD signal of ROIs was normalized (around their mean value) and categorized (binarized by replacing data higher than the mean value with the number 1 and those lower or equal to the mean value with the number 0). Thus, the functional profiles of all BG at any time point were represented by a single byte (each of the eight brain regions studied provided a 0 or a 1 to one of the 8 bits of the byte). The 'contingence table' was made with the representative bytes of the functional status of BG recorded during successive time intervals (1.6 s time resolution in this study). The number of times each particular BG profile was computed during the whole recording was then used to build the 'frequency table'. In this table, the BG profiles are ordered according to their relative frequency. The number of times that each profile was followed by each of the other profiles was introduced in the 'transition table', and profile transitions with a frequency higher than that expected at random were included in the 'transition matrix'. The χ^2 test was used to establish differences between the control group and the randomly simulated group or between the control group and the Parkinson's disease group, comparisons that were performed for both profiles and profile transitions. ROIs = regions of interest.

(S1), Put, external globus pallidum, subthalamic nucleus, internal globus pallidum, substantia nigra and Tal successively] whose binary numbers represented the low (0)/high (1) activity of particular BGmC areas. These functional bytes were included in a 'contingence table' (see Fig. 1C), which had all the BG profiles of each subject ordered according to their presentation (1.6 s between successive profiles). The number of times that each BG profile was found in the contingency table was then introduced in the 'frequency table' (see Fig. 1D), where each profile occupied a different row. Because the possible number of different functional status for a 1-byte profile is 256, this was also the number of rows in the frequency table. In this table, the BG profiles were ordered according to their relative frequency. Two expected profiles were computed, such as the theoretical profile and the simulated expected profile. The theoretical

profile assumes that all profiles are displayed at random, and that each particular profile will be found once every 256 profiles. Simulated profiles were computed by a random generation of the same number of profiles recorded in the actual study. For this simulation, the high (1) and low (0) status of each position of each profile byte was estimated by the random generation of a number between 0 and 1, with those numbers >0.5 being replaced by the number 1 and those <0.5 being replaced by the number 0. Ten contingency tables were simulated with this procedure, with the mean value of the number of times each profile was found in these simulated contingency tables being used to compute the simulated frequency table.

The number of times that each profile was followed by each of the other profiles was computed and entered in the 'transition table' (see Fig. 1E). Profiles that persisted for more than one time interval (>1.6 s) were recorded in

the transition table as self-transitions. The transition table has 256 rows (initial profiles) \times 256 columns (final profile), and the number of different possible transitions is 65 536 (for 1-byte profiles). The initial representation of the significant transitions was made with the Grafos programme (v1.3.5. by A. Rodriguez Villalobos).

Statistical analysis

The statistical significance of the presentation frequency of each profile was computed by a χ^2 test where the number of actual frequencies (found profiles) was contrasted with those expected at random (theoretical or simulated). The same procedure was used to establish statistical differences between the relative frequency of each profile in the control subjects (expected profiles) and patients with Parkinson's disease (found profiles). The statistical value of the number of transitions between each two particular profiles was computed by a χ^2 test where the number of actual transitions (found transitions) was contrasted with the number of the same transitions found in a succession of profiles computed by the simulation procedure commented above. The same χ^2 procedure was used to establish statistical differences between the relative frequency of each transition in control subjects (expected transitions) and patients with Parkinson's disease (found transitions).

Data availability

Anonymized data may be made available upon reasonable request to the corresponding author.

Results

The location of regions of interest ([Supplementary Table 1](#) shows the mean value and standard error for the studied persons) and the age of patients with Parkinson's disease (55.3 ± 7.2 years; mean \pm standard error) and controls (56.7 ± 8.2 years) showed no statistical differences. All patients with Parkinson's disease showed an early-to-mid clinical motor stage in the Hoehn and Yahr (1.50 ± 0.18 ; all patients had a scale stage of I or II), Unified Parkinson's Disease Rating Scale III (12.12 ± 1.61) and Schwab and England (92 ± 2.6) scales. Akinesia was the predominant symptom, with all patients showing an obvious delay in movement initiation and a low expression of tremor. Neither patients nor aged-matched controls showed dementia (Montreal Cognitive Assessment >26 and Mini-Mental State Examination >27) or abnormalities in the MRI studies. Data from one patient with Parkinson's disease and one control subject were excluded from the analysis due to excessive motion during the MRI recordings.

Profiles: the effect of Parkinson's disease

[Figure 2A and B](#) shows the distribution of the BG profiles in the control and Parkinson's disease groups, respectively (values represent the percentage of total profiles). The red lines show the distribution of the 256 possible profiles of actual data ordered from the most frequent—left side—to the less frequent—right side—profile (the x -axis shows the position of the profile according to its frequency and the y -axis shows the frequency of each profile as a percentage of total profiles—'relative frequency'). The blue lines show the same distribution but for randomly simulated profiles (these data were also ordered according to their frequency). The green lines show the probability values (P computed with a χ^2 test) found between the frequency of real and randomly simulated profiles. These figures show that the frequency of some BG profiles was much higher than that expected at random ($P < 0.0001$), whereas other profiles were seldom observed or never appeared ($P < 0.001$). This asymmetrical distribution of BG profiles was found in both the control and Parkinson's disease groups. This initial analysis shows that BG activity facilitates some BG profiles (co-variant profiles) but prevents others.

[Figure 2C](#) also shows the frequency of profiles, but now the x -axis shows the byte corresponding to each profile (from 00000000 to 11111111) in a decimal base (from 0 to 255) and the y -axis shows the relative frequency of profiles. The black line shows the distribution of simulated profiles (all $\sim 0.39\%$), the blue line shows the distribution of profiles in the control group, and the red lines show the distribution of profiles in the Parkinson's disease group. Both control and Parkinson's disease groups showed some profiles with a frequency much higher than that expected at random (peaks of [Fig. 2C](#)). The correlation of the frequency profiles of both groups ([Fig. 2D](#)) shows that profiles with the highest frequency in the control group were also those with the highest frequency in the Parkinson's disease group. However, a more detailed view of the frequency of profiles shows some differences between groups. [Figure 2E](#) presents the frequency order of the 50 most frequent profiles in controls and patients with Parkinson's disease. This figure shows that the four most frequent profiles in the control group were also the four most frequent profiles in the Parkinson's disease group. However, some profiles found in the 10 most frequent profiles of control subjects were observed in more posterior positions in the Parkinson's disease group and profiles that were less frequent in controls were observed within the most frequent profiles of patients with Parkinson's disease. These observations suggest that the relative frequency of covariant profiles of BG is not exactly the same in controls and patients with Parkinson's disease. This can also be observed in the central graph of [Fig. 3](#) where the relative frequency of profiles can be compared (profiles are

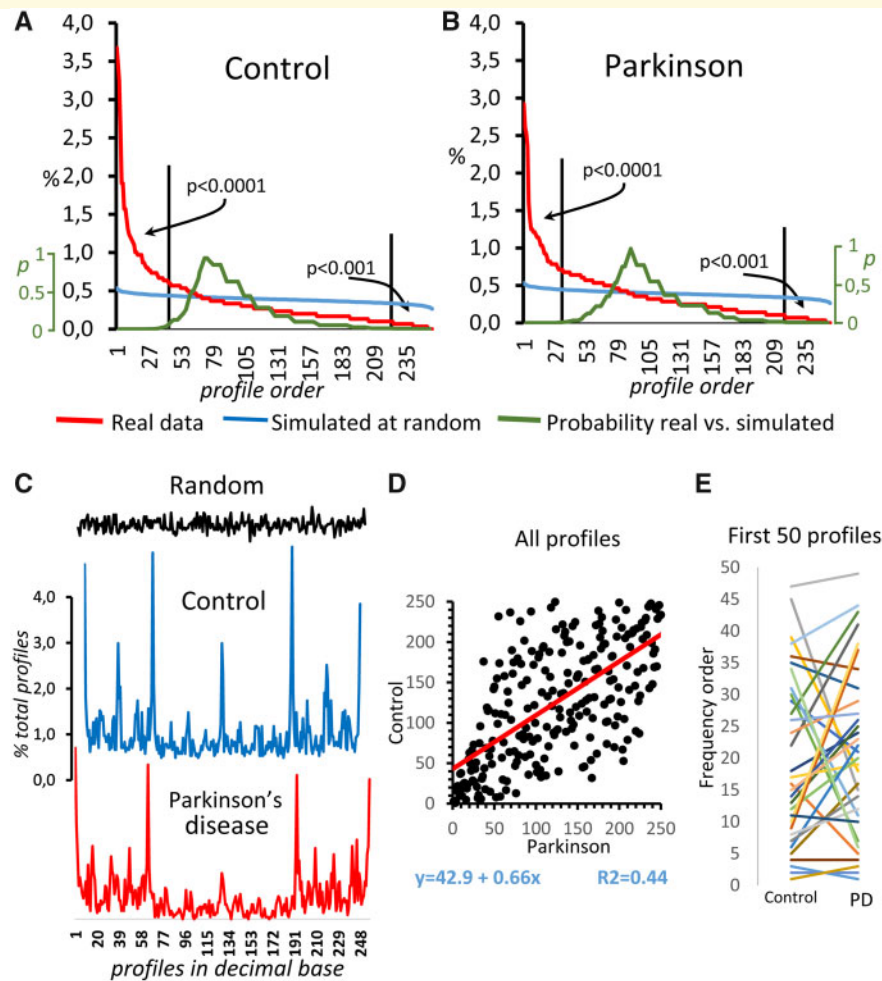


Figure 2 Distribution of BG profiles according to their relative frequency. (A and B) The distribution of the BG profiles in the control and Parkinson's disease groups, respectively (values represent the percentage of total profiles). The red lines show the distribution of actual profiles ordered from the most frequent—left side—to the less frequent—right side—profile. The blue lines show the same distribution but for randomly simulated profiles. The green lines show the probability values (P computed with a χ^2 test) found between the frequency of real and randomly simulated profiles. Whereas some profiles showed a frequency higher than that expected at random ($P < 0.0001$), others showed a frequency lower than that expected at random ($P < 0.001$). This asymmetrical distribution of BG profiles was found in both the control (A) and Parkinson's disease (B) groups. In C, the x-axis is the profile byte represented in a decimal base and the y-axis is the frequency of each profile as a percentage of total profiles (relative frequency). The black line shows the distribution of simulated profiles (all $\sim 0.39\%$), the blue line shows the distribution of profiles in the control group, and the red lines show the distribution of profiles in the Parkinson's disease group. (D) The control (y-axis) and Parkinson's disease (x-axis) relationship of profiles according to their position in the ranking of the most frequent profiles. (E) The frequency order of the 50 most frequent profiles in controls and patients with Parkinson's disease.

ordered according to their relative frequency in the control group). The high status of each BGmC region in each profile is indicated in the 'profile byte' by the number 1, and the low status is indicated by the number 0 (the position of each area in the profile byte is shown in the yellow square located in the centre of the figure). The frequency of profiles found in the control group is indicated with white circles, the frequency of profiles in the Parkinson's disease group is indicated with black circles and the frequency of random-simulated profiles is indicated with white triangles. All these high-frequency profiles showed, in both groups, a frequency higher than

that found in random-simulated profiles ($P < 0.0001$). The frequency of many of the first 10 profiles was higher in the control group than in the Parkinson's disease group (11000000, 00111111, 00011111, 10000000 and 11100001), and the frequency of most profiles between 16 and 25 was higher in the Parkinson's disease group than in the control group (e.g. 00000001, 11110100 and 11010000).

In the peripheral diagrams of the Fig. 3, the profile byte is accompanied by a picture, which includes the high-status regions within a brown area. For example, the profile byte 00111111 indicates that all BG are in a

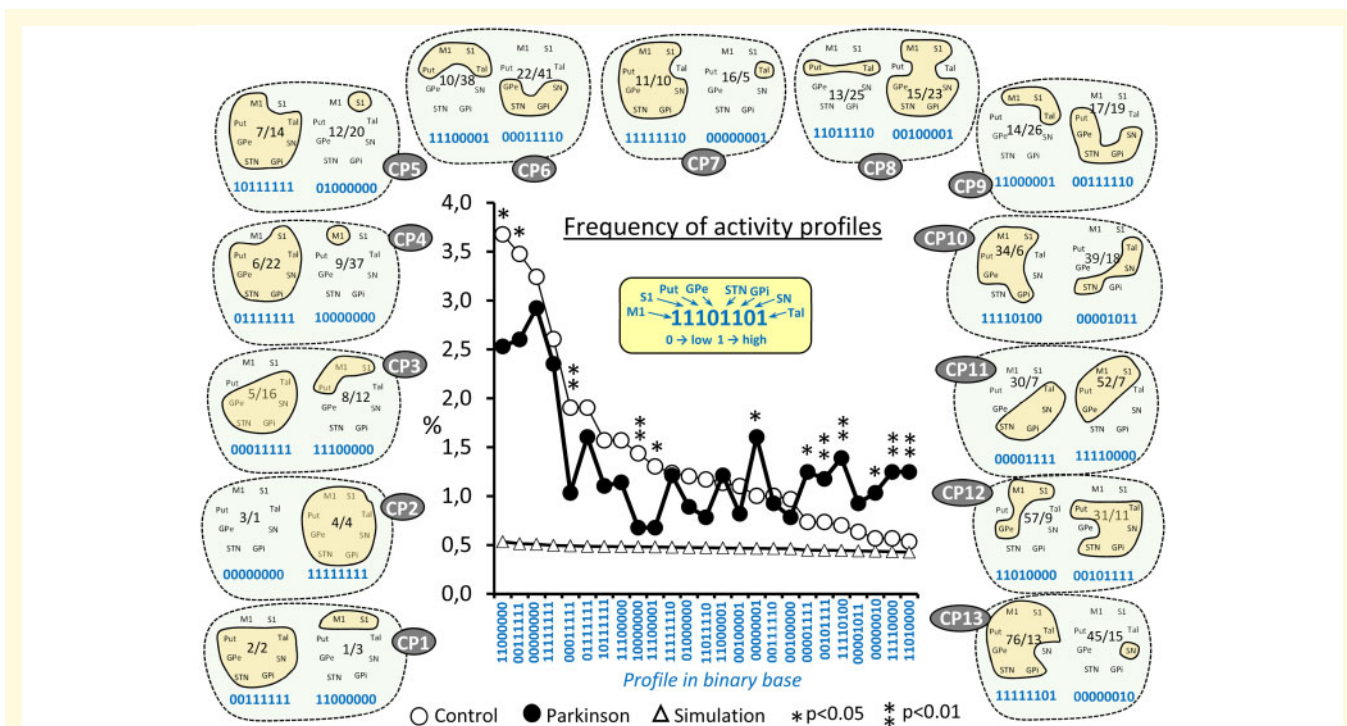


Figure 3 Frequency distribution of the most common BG profiles. The distribution of the most common profiles is shown in the centre (ordered according to their relative frequency in the control group). The frequency of each profile is indicated with white circles (control group), black circles (Parkinson group) and white triangles (random-simulated profiles). The profile byte shows the high/low status of each region in each profile (see the yellow square in the centre of the figure). In the peripheral diagrams, profile bytes are accompanied with a picture including the high-status areas within a brown area. In these pictures, profiles were grouped within green areas according to their complementary nature (CPs are those showing exactly opposite high/low status). Numbers included inside each peripheral picture indicate the frequency order of the profile byte in the control (first number) and Parkinson's disease (second number) groups. GPe = external globus pallidum; STN = subthalamic nucleus; GPi = internal globus pallidum; SN = substantia nigra.

high status and cortical areas in a low status, 11000000 indicates that all BG are in a low status and cortical areas are in a high status, 00000000 indicates that all areas are in a low status and 11100000 indicates that M1, S1 and Put are in a high status and the other areas are in a low status. These diagrams also include the frequency position of each profile. The numbers included in the pictures of each profile indicate the frequency order of profiles in the control group (left-side number) and in the Parkinson's disease group (right-side number). For instance, the 11000000 profile was in the first frequency position in the control group and in the third frequency position in the Parkinson's disease group, which agrees with the fact that the frequency of this profile was higher in controls than in patients with Parkinson's disease. The 00000001 profile, another example, occupied the frequency 16 in controls and 5 in patients with Parkinson's disease, which agrees with the higher frequency found for this profile in the Parkinson's disease group than in the control group.

A striking and unexpected finding was that practically all high-frequency profiles showed a complementary high-frequency profile with exactly the opposite high/low

status of their BG areas [complementary profile (CP)]. In the peripheral diagrams of Fig. 3, CPs are grouped within green areas limited by a dashed line. 11000000/00111111 profiles and 11111111/00000000 profiles, the four most frequent profiles, were grouped within CP1 and CP2, respectively. The profiles grouped in other CPs did not always have a similar frequency and their frequency position was not always consecutive (e.g. the position of the 10111111 and 01000000 CPs in the control group was 7 and 12, respectively).

Transitions between profiles: the effect of Parkinson's disease

Profiles showed complex successions (transitions) whose dynamic is not obvious with direct observation (Supplementary Video 1 shows an example of the dynamic of the profile transitions recorded in a subject of the control group). The first step to study transitions was to classify profiles according to their input/output transitions. The following three main profiles were identified: the 'input profile' showing high-frequency and statistically significant output transitions to other particular profiles

($P < 0.001$) but not significant input transitions coming from other areas of the BGmC, the ‘output profile’ showing input but not output high-frequency transitions and the ‘internal profile’ showing both input and output high-frequency transitions. Most internal profiles showed input transitions from input profiles, output transitions to output profiles and input and output transitions with other internal profiles. No significant transitions were found between random-simulated profiles.

Profile transitions with statistical value ($P < 0.001$) are indicated by arrows in Fig. 4, where they project from an origin profile to a destination profile. Some input profiles showed direct transitions to output profiles, thus bypassing the internal profiles (bypass transitions). Figure 4A and B presents the bypass transitions in controls and patients with Parkinson’s disease, respectively. Although the number of input profiles (4 in controls and 6 in patients with Parkinson’s disease), output profiles (9 in controls and 7 in patients with Parkinson’s disease) and bypass transitions (10 in controls and 10 in patients with Parkinson’s disease) was similar in both groups, the origin profile and destination profile of transitions, which reached statistical significance, were different in the control and Parkinson’s disease groups. Only one input profile (00000001) and two output profiles (00000000 and

11111111) reached statistical value in both groups. Figure 4C and D presents the input (red arrows) and output (green arrows) transitions of internal profiles. The input profiles (pink circles) showing three or more transitions to internal profiles will be referred to below as ‘hub input profiles’ (white circles). The number of input profiles with transitions to the internal profiles (yellow circles) decreased in patients with Parkinson’s disease with respect to controls (decreased from 5 to 3 transitions), a fact that also occurred with the hub of input profiles, which decreased from 2 to 1. The number of transitions from input profiles to internal profiles (red arrows) decreased from 13 in controls to 5 in patients with Parkinson’s disease. However, the number of transitions from internal profiles to output profiles (green circles) increased from 18 in controls to 25 in patients with Parkinson’s disease (green arrows). These data suggest that internal profiles of patients with Parkinson’s disease received less input transitions but sent more output transitions than controls. 11111111 and 00000000 output profiles received three or more transitions in both control and patients with Parkinson’s disease (most other output profiles received only one transition), being referred to below as ‘hub output profiles’ (cyan circles). Because the high density of transitions between internal

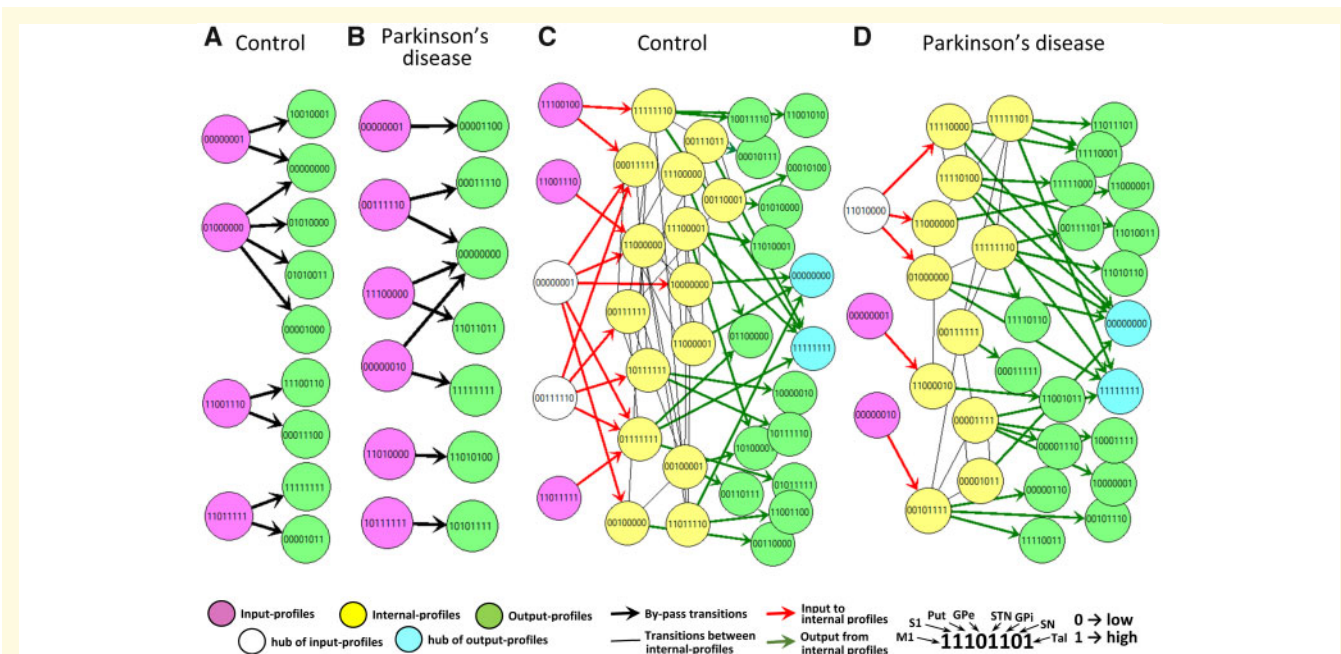


Figure 4 Profile transitions in the control (A and C) and Parkinson’s disease (B and D) groups. Profile transitions with statistical value ($P < 0.001$) are shown with arrows, which project from the origin profile to the destination profile. Input profiles are included within pink circles, output profiles are included within green circles and internal profiles are included within yellow circles. Input profiles showing three or more transitions to internal profiles (hub input profiles) are shown within white circles, and output profiles receiving three or more transitions from internal profiles (hub output profiles) are shown within cyan circles. Bypass transitions directly connecting input and output profiles are shown with black arrows in A and B. Input transitions connecting input profiles with internal profiles are shown with red arrows in C and D. Output transitions connecting internal profiles with output profiles are shown with green arrows in C and D. Internal transitions connecting some internal profiles with others are shown by thin black lines in C and D. The high/low status of each region in profile bytes is indicated according to the position shown in the bottom-right corner of the figure.

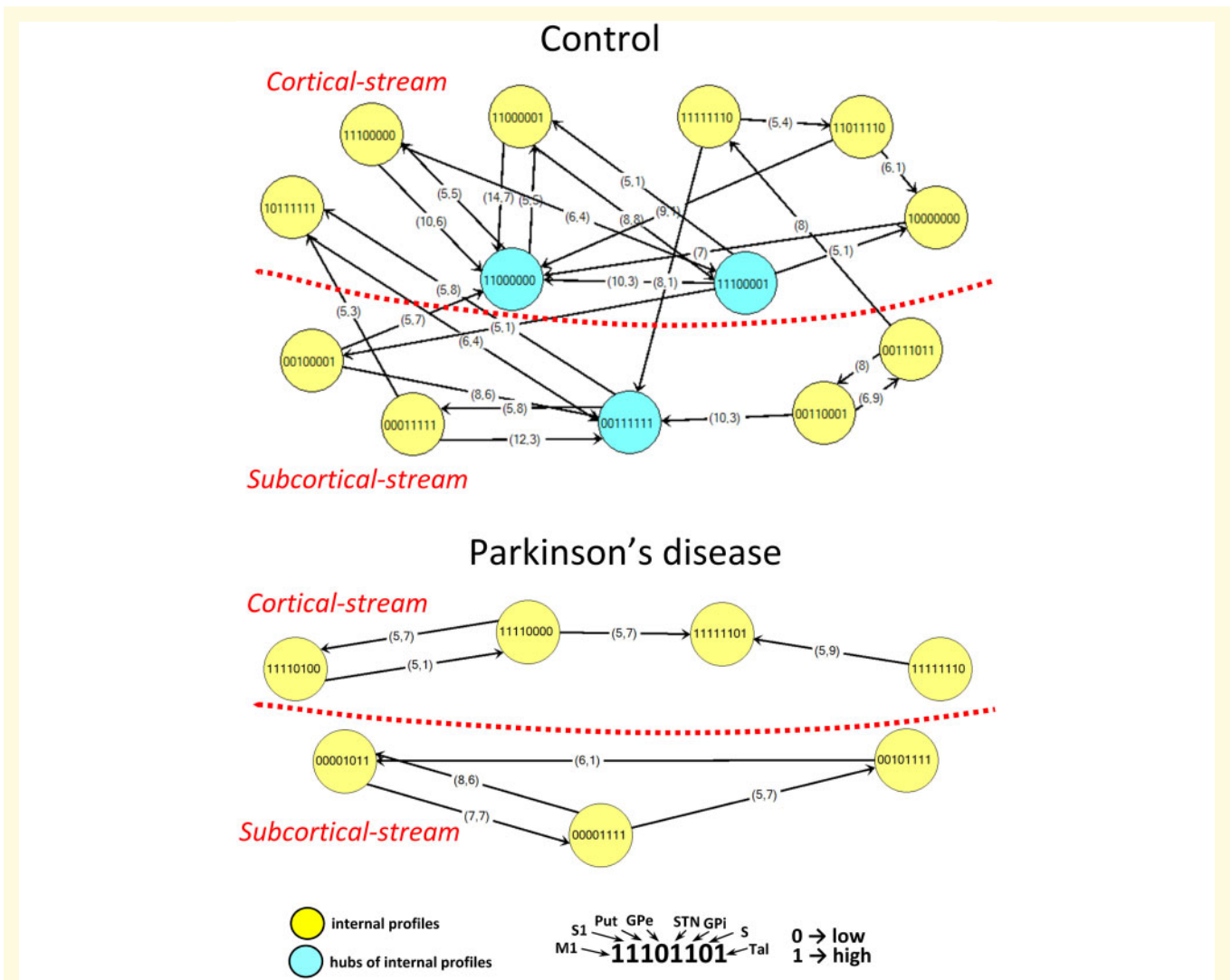


Figure 5 Profile transitions between internal profiles in the control (top) and Parkinson's disease (bottom) groups. Profile transitions with statistical value ($P < 0.001$) are shown with arrows, which project from the origin profile to the destination profile. Internal profiles are included within pink circles, but those internal profiles showing more than three transitions (hub internal profiles) are shown within cyan circles. Transitions between profiles with activation of cortical regions (cortical stream) are shown above the red-dotted line, and transitions between profiles without activation of cortical regions (subcortical stream) are shown below the red-dotted line. The number of arrows shows the percentage of all transitions generated from the origin profile, which projected to the target profile of the arrow. The high/low status of each region in profile bytes is indicated according to the position shown in the bottom-right corner of the figure.

profiles (internal transitions) hinders their perception in this figure, they are represented with thin black lines and may be better observed in Fig. 5.

Figure 5 shows the internal transitions in controls (top) and patients with Parkinson's disease (bottom). Internal profiles are shown within yellow circles except for those with more than five transitions, which are shown within cyan circles and will be referred to below as 'hub of internal profiles'. Profiles with activation of cortical regions are located above the red-dotted line of this figure (cortical stream), and those with non-active cortical areas are located below the red-dotted line (subcortical stream). The number included in each arrow indicates the relative

relevance of the transition (it shows the percentage of all transitions generated from the origin profile, which projected to the target profile of the arrow). For instance, the 11000001 → 11000000 transition represents 14.7% of all transitions originating from the 11000001 profile (transitions between random-simulated profiles are ~0.39%). Patients with Parkinson's disease showed a low number of internal profiles and a very low number of internal transitions regarding control subjects (Fig. 5, bottom). Thirteen internal profiles were found in the control group, while only seven internal profiles reached statistical significance in the Parkinson's disease group. The number of internal transitions with statistical significance was

26 in controls and 8 in patients with Parkinson's disease. The number of internal-profile hubs was 3 in controls and 0 in patients with Parkinson's disease. Nine internal profiles showed reciprocal transitions in the control group, a number that decreased to 4 in patients with Parkinson's disease. Finally, all the internal profiles of controls were directly or indirectly connected by internal transitions. These 'trans-streams transitions' were not found in patients with Parkinson's disease, who showed a full segregation of the cortical (located above the red line in Fig. 5) and subcortical (located below the red line in Fig. 5) streams.

Discussion

The present work examined the physiological activity of the human BGmC with fcMRI and the FPM, which is a new analytical approach. The FPM identified a number of multiple co-activations of BG (profiles), which displayed an intricate time dynamic (profile transitions) previously unobserved with other methods. Both the frequency of profiles and the dynamic of profile transitions showed marked disruptions in patients with Parkinson's disease.

Methodological considerations

Although MCA has several advantages to study the global dynamic of BG (Rodriguez-Sabate et al., 2017a, 2019a), there are some limitations that constrain its success. MCA can only identify a portion of BG interactions (seven global interactions in our previous study), it does not provide information about the functional dynamic of BG and it is an exploratory method without statistical verification of results (Rodriguez-Sabate et al., 2017a, 2019a). The FPM overcomes these limitations, identifying with statistical criteria a number of different functional associations of BGmC areas (profiles) and showing a dynamic view of the BG activity (profile transitions) not provided by MCA or other multivariate methods. However, the FPM also has some limitations that should be taken into account in fcMRI studies. The time resolution and space resolution of fcMRI prevent the FPM from studying the fast interactions of small populations of cells, and so neither the fast excitatory/inhibitory interactions nor the structural connections of BG can be studied with fcMRI/FPM. The FPM can identify the co-activations of BG regions (profiles) and the time successions between these profiles (profile transitions), which appear with a frequency higher than that expected at random. It would be interesting to establish relationships between the present model and the closed-loop model of BG, and some of the following comments show our interest in doing this. However, both models describe BG activity from a different point of view and these comments should be considered as possible associations but not as

proof of direct relationships between both functional perspectives.

Profiles and profile transitions in the basal ganglia motor circuit

'11000000' (cortical areas activated and BG inactivated) and '00111111' (cortical areas inactivated and BG activated) were the most frequent profiles of the BGmC. These profiles correspond with the functional configurations previously isolated in the first and second dimensions of MCA, the two most relevant dimensions for this analytical method (Rodriguez-Sabate et al., 2019a). 11000000 and 00111111 profiles had a complementary distribution (CP1), a puzzling fact also found in other high-frequency profiles (CP2 to CP13). The finding of complementarity profiles could be associated to some kind of rebound response, which substitutes the high/low functional status of BG for its opposite status. However, CPs never showed significant transitions between one another, which do not support this hypothesis. In fact, 11000000 and 00111111 behaved as a hub for internal profiles, displaying numerous transitions with other internal profiles and no direct transitions between them (Fig. 5, top). The global dynamic of the internal profiles of BGmC was segregated in two main components: a cortical stream around the 11000000 (and 11100001) and a subcortical stream around the 00111111. Although the profiles of these streams showed preferred transitions with other profiles of the same stream, they also displayed transitions to profiles of the other stream (trans-stream transitions), suggesting that information flows between both streams.

The '00000000' (all the BCmC inactivated) and '11111111' (all the BCmC activated) CPs (CP2) were the third and fourth most frequent profiles, working as output-profile hubs that received the highest number of transitions. With the exception of 11111111 and 00000000 profiles, practically all the other output profiles only received a single transition from the internal profiles, a fact observed in controls (Fig. 4C) and patients with Parkinson's disease (Fig. 4D). 11111111 and 00000000 received transitions from several internal profiles of both streams, thus working as a common way out for the information processed by any of the internal profile streams.

'CP3' and 'CP9' present alternating activations of the cortical areas and BG. These cortical activations were accompanied by the synchronous activation of the Put (CP3) or the thalamus (CP9). Bearing in mind the structural relationships between the cortex and BG, the CP3 profiles could be involved in the arrival of cortical information to the BG and the CP9 profiles could be involved in the return of BG information to the cortex. 'CP6' and 'CP8' provide an alternative way to relate the input/output centres of BG with the other regions of the BGmC. CP8 shows an alternation between a Put/Tal co-activation

(with the other inactive BGmC regions) and a Put/Tal co-inactivation (with the other active regions), which could involve the excitatory Tal \rightarrow Put projection. CP6 shows an alternation in the co-activation/co-inactivation of Put/Tal/M1/S1, which could be linked to the excitatory projection from the Tal to the cortex and from the cortex to external globus pallidum. Thus, the input–output centres of BG may be functionally linked in two main ways, one using direct projections (CP8) and the other using indirect projections through the cortex (CP6). However, and as commented above, these are only possible relationships between the excitatory–inhibitory closed-loop model of BG and the present co-activation model and no proof of these relationships is provided here.

Profile transitions in Parkinson's disease

Control subjects showed massive transitions between the internal profiles of the cortical and subcortical streams (six transitions), a fact not observed in patients with Parkinson's disease whose internal-profile hubs disappeared and whose transitions between cortical and subcortical streams vanished. These findings and the marked reduction in the number of internal profiles observed in patients with Parkinson's disease suggest a profound effect of Parkinson's disease on the covariant activity of BG. These differences were observed in patients with few motor disorders suggesting that the fMRI/FPM method could be useful for the early diagnosis of Parkinson's disease.

The particular role of each profile transition in the BG functions and in the motor and non-motor disorders of Parkinson's disease needs further specific studies. The BGmC is involved in different functions including the selection of motor tasks, the control of different reflexes or the modulation of the muscle tone, functions that are also performed in subjects at rest (Cham *et al.*, 2007; Schwarz and Peever, 2011; Fearon *et al.*, 2015; Mellone *et al.*, 2016). The specific procedures used by the BGmC nuclei to perform these tasks are presently unknown, and they could involve alterations in the assembly of profiles or in the preparation of profile transitions. Functional profiles could be associated with particular tasks. During daily living activities, people are normally fluctuating between different mental and motor tasks, a fact that also occurs in resting people and during the realization of MRI studies (e.g. modulation of muscle tone, reflexes and body posture). Thus, it is possible that the incidental involuntary activation of these tasks may be associated with the fluctuation of functional profiles observed here. Many Parkinson's disease disorders that are present during the resting intervals (hypertonia, tremor, dysreflexia, alterations of different mental functions, etc.; Wright *et al.*, 2007; Lucza *et al.*, 2015; Mellone *et al.*, 2016; Weil *et al.*, 2019) could be associated with the restriction

of functional profiles and profile transitions observed here in patients with Parkinson's disease.

Basal ganglia as a covariant network

The new method introduced here proved useful to study the multiple covariant behaviour of human BG. The analysis of covariance has proved successful to study different complex systems and is the main methodological tool in disciplines as consolidated as quantum electrodynamics and molecular biology or as promising as quantum gravity (Shen and Li, 2016). This approach is particularly useful when it is not possible to access all the variables that are involved in the process under study, a fact that clearly occurs in the human brain. BG are composed of many millions of neurons, each of which are interconnected with hundreds of other neurons by thousands of synapses and millions of receptors. The system is enormously complex and its individual components cannot be currently monitored and will probably not be monitored for many years. Thus, we are obliged to use simplified models suitable for making reliable estimates of BG activity.

Covariant models describe the behaviour of complex systems as changes in the functional arrangement of their variables or components, which is represented here by the profile transitions. The present multiple covariant model of BG is based on data directly obtained from the human brain, providing actual probabilities for the transitions performed between each of the possible functional profiles of the system. These advantages are obtained at the expense of a marked reduction and simplification of the BG networks. Instead of bioelectric signals, we used the BOLD signals that are indirect indicators of energy consumption of brain areas. Thus, it is assumed that brain nuclei involved in the processing of current information need more energy and can be identified with the BOLD signal. To record the BOLD signal from hundreds of thousands of places in the brain requires long time intervals, even for such advanced technologies such as MRI. Thus, this covariant model is based on the slow fluctuation of brain activity that persists for 1.6 s or more. Most behavioural patterns require several seconds to complete (e.g. to say something or to write a note in the mobile), but they involve a number of sub-tasks, which may be done in fractions of a second and that are performed in time intervals shorter than the temporal resolution of the MRI. Thus, the covariant model does not provide information about the mechanisms involved in the sub-components of particular tasks. It only can provide information about the involvement of particular functional conformations (profiles) of the brain areas of a network in a particular task. As commented above, the parkinsonian brain shows marked changes in the frequency of profiles and profile transitions. Another potential use of the covariant model of BG could be the

diagnosis and prognosis of the clinical evolution of Parkinson's disease, and perhaps the identification of profiles and profile transitions involved in its clinical disturbances.

Supplementary material

Supplementary material is available at *Brain Communications* online.

Acknowledgments

The authors thank the neurologists Fernando Monton and Jesus N. Lorenzo for their assistance in the Parkinson's disease diagnosis.

Funding

This study was funded by the Center for Networked Biomedical Research in Neurodegenerative Diseases (CIBERNED), Madrid, Spain (grant number PI2014/06).

Competing interests

The authors report no competing interests.

References

- Albin RL, Young AB, Penney JB. The functional anatomy of basal ganglia disorders. *Trends Neurosci* 1989; 12: 366–75.
- Alexander GE, DeLong MR, Strick PL. Parallel organization of functionally segregated circuits linking basal ganglia and cortex. *Annu Rev Neurosci* 1986; 9: 357–81.
- Arthurs OJ, Boniface S. How well do we understand the neural origins of the fMRI BOLD signal? *Trends Neurosci* 2002; 25: 27–31.
- Canavan AG, Nixon PD, Passingham RE. Motor learning in monkeys (*Macaca fascicularis*) with lesions in motor thalamus. *Exp Brain Res* 1989; 77: 113–26.
- Cazorla M, de Carvalho FD, Chohan MO, Shegda M, Chuhma N, Rayport S, et al. Dopamine D2 receptors regulate the anatomical and functional balance of basal ganglia circuitry. *Neuron* 2014; 81: 153–64.
- Cui G, Jun SB, Jin X, Pham MD, Vogel SS, Lovinger DM, et al. Concurrent activation of striatal direct and indirect pathways during action initiation. *Nature* 2013; 494: 238–42.
- Cham R, Perera S, Studenski SA, Bohnen NI. Striatal dopamine denervation and sensory integration for balance in middle-aged and older adults. *Gait Posture* 2007; 26: 516–25.
- Damoiseaux JS, Rombouts SA, Barkhof F, Scheltens P, Stam CJ, Smith SM, et al. Consistent resting-state networks across healthy subjects. *Proc Natl Acad Sci USA* 2006; 103: 13848–53.
- DeLong MR. Primate models of movement disorders of basal ganglia origin. *Trends Neurosci* 1990; 13: 281–5.
- DeLong M, Wichmann T. Update on models of basal ganglia function and dysfunction. *Parkinsonism Relat Disord* 2009; 15 (Suppl 3): S237–40.
- Eklund A, Knutsson H, Nichols TE. Cluster failure revisited: impact of first level design and physiological noise on cluster false positive rates. *Hum Brain Mapp* 2018; 40: 2017–32.
- Fearon C, Doherty L, Lynch T. How do I examine rigidity and spasticity? *Mov Disord Clin Pract* 2015; 2: 204.
- Fox MD, Raichle ME. Spontaneous fluctuations in brain activity observed with functional magnetic resonance imaging. *Nat Rev Neurosci* 2007; 8: 700–11.
- Goebel R, Esposito F, Formisano E. Analysis of functional image analysis contest (FIAC) data with brainvoyager QX: from single-subject to cortically aligned group general linear model analysis and self-organizing group independent component analysis. *Hum Brain Mapp* 2006; 27: 392–401.
- Ikemoto S, Yang C, Tan A. Basal ganglia circuit loops, dopamine and motivation: a review and enquiry. *Behav Brain Res* 2015; 290: 17–31.
- Jo HJ, Gotts SJ, Reynolds RC, Bandettini PA, Martin A, Cox RW, et al. Effective preprocessing procedures virtually eliminate distance-dependent motion artifacts in resting state fMRI. *J Appl Math* 2013; 2013: 1.
- Kravitz AV, Freeze BS, Parker PR, Kay K, Thwin MT, Deisseroth K, et al. Regulation of parkinsonian motor behaviours by optogenetic control of basal ganglia circuitry. *Nature* 2010; 466: 622–6.
- Lee K, Tak S, Ye JC. A data-driven sparse GLM for fMRI analysis using sparse dictionary learning with MDL criterion. *IEEE Trans Med Imaging* 2011; 30: 1076–89.
- Logothetis NK. The neural basis of the blood-oxygen-level-dependent functional magnetic resonance imaging signal. *Phil Trans R Soc Lond B* 2002; 357: 1003–37.
- Logothetis NK, Wandell BA. Interpreting the BOLD signal. *Annu Rev Physiol* 2004; 66: 735–69.
- Lucza T, Karadi K, Kallai J, Weintraut R, Janszky J, Makkos A, et al. Screening mild and major neurocognitive disorders in Parkinson's disease. *Behav Neurol* 2015; 2015: 1.
- Marceglia S, Foffani G, Bianchi AM, Baselli G, Tamma F, Egidio M, et al. Dopamine-dependent non-linear correlation between subthalamic rhythms in Parkinson's disease. *J Physiol* 2006; 571: 579–91.
- McCutcheon RA, Abi-Dargham A, Howes OD. Schizophrenia, dopamine and the striatum: from biology to symptoms. *Trends Neurosci* 2019; 42: 205–20.
- McHaffie JG, Stanford TR, Stein BE, Coizet V, Redgrave P. Subcortical loops through the basal ganglia. *Trends Neurosci* 2005; 28: 401–7.
- Mellone S, Mancini M, King LA, Horak FB, Chiari L. The quality of turning in Parkinson's disease: a compensatory strategy to prevent postural instability? *J Neuroeng Rehabil* 2016; 13: 39.
- Neumann WJ, Schroll H, de Almeida Marcelino AL, Horn A, Ewert S, Irmen F, et al. Functional segregation of basal ganglia pathways in Parkinson's disease. *Brain* 2018; 141: 2655–69.
- Olszowy W, Aston J, Rua C, Williams GB. Accurate autocorrelation modeling substantially improves fMRI reliability. *Nat Commun* 2019; 10: 1220.
- Power JD, Mitra A, Laumann TO, Snyder AZ, Schlaggar BL, Petersen SE. Methods to detect, characterize, and remove motion artifact in resting state fMRI. *Neuroimage* 2014; 84: 320–41.
- Raichle ME. Behind the scenes of functional brain imaging: a historical and physiological perspective. *Proc Natl Acad Sci USA* 1998; 95: 765–72.
- Raichle ME, Mintun MA. Brain work and brain imaging. *Annu Rev Neurosci* 2006; 29: 449–76.
- Redgrave P, Marrow L, Dean P. Topographical organization of the nigroreticular projection in rat: evidence for segregated channels. *Neuroscience* 1992; 50: 571–95.
- Rodriguez M, Gonzalez J, Sabate M, Obeso J, Pereda E. Firing regulation in dopaminergic cells: effect of the partial degeneration of nigrostriatal system in surviving neurons. *Eur J Neurosci* 2003a; 18: 53–60.

- Rodriguez M, Pereda E, Gonzalez J, Abdala P, Obeso JA. How is firing activity of substantia nigra cells regulated? Relevance of pattern-code in the basal ganglia. *Synapse* 2003b; 49: 216–25.
- Rodriguez M, Pereda E, Gonzalez J, Abdala P, Obeso JA. Neuronal activity in the substantia nigra in the anaesthetized rat has fractal characteristics. Evidence for firing-code patterns in the basal ganglia. *Exp Brain Res* 2003c; 151: 167–72.
- Rodriguez-Sabate C, Llanos C, Morales I, Garcia-Alvarez R, Sabate M, Rodriguez M. The functional connectivity of intralaminar thalamic nuclei in the human basal ganglia. *Hum Brain Mapp* 2015; 36: 1335–47.
- Rodriguez-Sabate C, Morales I, Lorenzo JN, Rodriguez M. The organization of the basal ganglia functional connectivity network is non-linear in Parkinson's disease. *Neuroimage Clin* 2019a; 22: 101708.
- Rodriguez-Sabate C, Morales I, Monton F, Rodriguez M. The influence of Parkinson's disease on the functional connectivity of the motor loop of human basal ganglia. *Parkinsonism Relat Disord* 2019b; 63: 100–105.
- Rodriguez-Sabate C, Morales I, Sanchez A, Rodriguez M. The multiple correspondence analysis method and brain functional connectivity: its application to the study of the non-linear relationships of motor cortex and basal ganglia. *Front Neurosci* 2017a; 11: 345.
- Rodriguez-Sabate C, Sabate M, Llanos C, Morales I, Sanchez A, Rodriguez M. The functional connectivity in the motor loop of human basal ganglia. *Brain Imaging Behav* 2017b; 11: 417–29.
- Schroll H, Hamker FH. Computational models of basal-ganglia pathway functions: focus on functional neuroanatomy. *Front Syst Neurosci* 2013; 7: 122.
- Schwarz PB, Peever JH. Dopamine triggers skeletal muscle tone by activating D1-like receptors on somatic motoneurons. *J Neurophysiol* 2011; 106: 1299–309.
- Shen W, Li Y. A novel algorithm for detecting multiple covariance and clustering of biological sequences. *Sci Rep* 2016; 6: 30425.
- Soares J, Kliem MA, Betarbet R, Greenamyre JT, Yamamoto B, Wichmann T. Role of external pallidal segment in primate parkinsonism: comparison of the effects of 1-methyl-4-phenyl-1,2,3,6-tetrahydropyridine-induced parkinsonism and lesions of the external pallidal segment. *J Neurosci* 2004; 24: 6417–26.
- Su X, Wijayasinghe CS, Fan J, Zhang Y. Sparse estimation of Cox proportional hazards models via approximated information criteria. *Biometrics* 2016; 72: 751–9.
- Weil RS, Winston JS, Leyland LA, Pappa K, Mahmood RB, Morris HR, et al. Neural correlates of early cognitive dysfunction in Parkinson's disease. *Ann Clin Transl Neurol* 2019; 6: 902–12.
- Wright WG, Gurfinkel VS, Nutt J, Horak FB, Cordo PJ. Axial hyper-tonicity in Parkinson's disease: direct measurements of trunk and hip torque. *Exp Neurol* 2007; 208: 38–46.
- Yin HH. Action, time and the basal ganglia. *Phil Trans R Soc B* 2014; 369: 20120473.
- Yin HH. The basal ganglia in action. *Neuroscientist* 2016; 23: 299–313.
- Zhang D, Snyder AZ, Shimony JS, Fox MD, Raichle ME. Noninvasive functional and structural connectivity mapping of the human thalamocortical system. *Cereb Cortex* 2010; 20: 1187–94.